Int. J. Environ. Sci. Technol. (2016) 13:339–348
DOI 10.1007/s13762-015-0890-2

ORIGINAL PAPER

Analytical investigation of CO_2 sensor based on carbon strand

E. Akbari[1] · Z. Buntat[1] · A. Afroozeh[2] · A. Zeinalinezhad[3] · M. Khaledian[4]

Received: 2 March 2015 / Revised: 13 September 2015 / Accepted: 21 September 2015 / Published online: 5 November 2015

Abstract This experimental study attempts to design and develop a novel carbon-based material fabrication method that implements high voltage AC arc discharge. The carbon-based material is to be used in an electric circuit to build up a gas sensing mechanism. After applying a high AC voltage to the graphite electrodes employed in the experiment, an arc ignites between the electrodes as the gas between them is iodized. In the carbon decomposition process, the arc is employed and results in the fabricated carbon strands. Thereafter, carbon monoxide (CO_2) in the atmospheric pressure is passed over the electrodes in the Pyrex glass tube chamber where the carbon strand fabrication process takes place. An increment appears in the measured current voltage (*I–V*) between the two sides of the carbon strand as the carrier concentration of CO_2 gas is increased from 200 to 800 ppm. Support vector regression (SVR) algorithm was used for data processing with statistical analysis for errors and quality control.

Keywords AC arc discharge · CO_2 gas sensor · Support vector regression (SVR) · *I–V* characteristics

✉ E. Akbari
elnazzz1@gmail.com

[1] Faculty of Electrical Engineering, Institute of High Voltage & High Current, Universiti Teknologi Malaysia, Johor Bahru, Malaysia

[2] Young Researchers and Elite Club, Jahrom Branch, Islamic Azad University, Jahrom, Iran

[3] Chemistry Department, Anar Branch, Islamic Azad University, Anar, Iran

[4] Department of Electronic Engineering, Faculty of Electrical Engineering, Universiti Teknologi Malaysia, 81310 Skudai, Johor, Malaysia

Introduction

The planet Earth is being depleted of its precious resources. As industries discover new resources for development, the environment and human habitat become vulnerable to serious changes (Gupta et al. 2012, 2013). However, methane (CH_4) makes up only 9 % of anthropogenic greenhouse gases, but it has 86 times global warming potential of CO_2 (Gupta and Saleh 2013; Huttunen et al. 2003). Similarly, carbon gives an effect biology, but industrial electronics are based on silicon technology (Akbari et al. 2014a; Davidson et al. 2004). Geology and biology of our existence on the planet Earth is greatly affected by both silicon and carbon effects. This paper truly focuses on industrial system giving directions for development of total quality management (TQM) with a prototype detection of methane. Consequently, industrial environmental engineering is becoming challenging from both professional and ethical points of view. Innovations, inventions, and growth naturally arise as industrial professionals design and implement new systems using existing science.

Accordingly, sensors or detection devices are required to sense gaseous threats and chemical warfare. Some of these elements are difficult to detect with our naked eye, but slowly they build up adverse effect on our ecosystem (Akbari et al. 2014b). Clearly, gas, chemical, and biosensors are general types of sensors that are commonly used for industry in everyday life applications. Thus, "(Akbari et al. 2013) provided model for gas sensor." This paper is contributed by developing a novel technique for the carbon

film fabrication implementing AC arc discharge. This carbon-based material has been intended to be used in a gas sensing mechanism. Subsequently, the process of carbon strand fabrication occurs in the Pyrex glass tube chamber when pure methane is passed through the graphite electrodes under atmospheric pressure.

Apparently, the chemical composition of methane (CH_4) comprises of carbon (C) and hydrogen (H) in a molar ratio of 1:4. Hence, when the graphite electrodes in the experiment are provided with a relatively high voltage, an electromagnetic field is created in the arc zone between them, which increases the acceleration of the electrons to a much greater speed beyond their normal movements (Schoell 1980; Stevens and Engelkemeir 1988). In a situation of high voltage, arc discharges under a continuous flow of methane. The intense field causes collisions between the electrons and gas molecules within the arc zone. In the collision process, subsequent energy transfer occurs from the energized electrons to neutral atoms and provides large number of free electrons. Therefore, continuous current supply boosts the interaction between neutral gas species and these free electrons. The number of interactions is a function of gas pressure as well as its degree of ionization. In addition, further supply of current gradually increases the voltage in the arc zone that causes CH_4 to break down to its constituent components. The isolated carbon atoms cause nucleation and merge together in the gap between the two electrodes (Craig et al. 1988).

Materials and methods

The experimental setup

An illustration of the complete experimental setup assembly employed in high voltage AC arc discharge generation is provided below in Fig. 1.

As illustrated in the schematic diagram, the Pyrex glass tube made of two Teflon flanges is used for reactor chamber fabrication with one side connected to a gas bubbler for toxin gas absorption and the other side connected to a gas flow controller. Then, methane gas at a constant flow of 0.2–1.0 (SLPM) was passed over the chamber, and a regulator is used to control the flow of methane gas and the atmospheric pressure. To start the methane decomposition procedure, the neon transformer with 50 Hz operation frequency was applied to the graphite electrodes. A high-voltage probe was coupled to oscilloscope in order to observe the applied voltage.

However, in order to avoid any possible explosion, methane was flushed through the reactor chamber for 1 min to make sure there is no ambient air present before applying high voltage. Consequently, in the presence of methane flow, when the high voltage was applied, arc discharge occurred causing the gas to decompose into its constituent elements, thus leaving a minute strand of carbon soot with extremely small thickness between the two electrodes. The structural morphology of the resulting

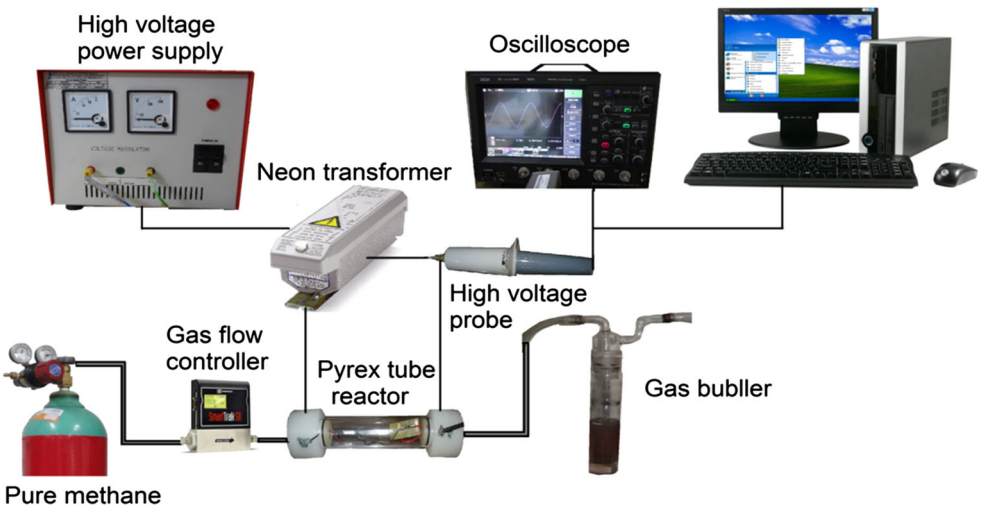

Fig. 1 Schematic of carbon film fabrication procedure

Table 1 Carbon strand fabrication parameters

Parameters	Value
High voltage	1–26 kV
Gas	Pure methane
Frequency	50 Hz
Temperature	At room environment
Flow rate	0.2–1.0 SLPM
Pressure	Atmospheric

carbon strand was investigated by scanning electron microscopy (SEM) and high-resolution optical microscope. The carbon film fabrication factors are shown in Table 1.

Effectively, the arc discharge method in the experimental study allows for a more cost-effective carbonaceous material production as no catalysts were used in the fabrication process. The outstanding electrical properties in the obtained materials make them ideal and promising for application in sensors. Furthermore, the high voltage arc discharge method employed in the fabrication process using pure methane makes it possible to obtain carbon strands as well as hydrogen gas. This approach can be further improved to allow for mass production of both materials in one single process, thereby reducing the fabrication/production costs.

Also, the methane decomposition and carbon deposition process result in a minute soot of carbon atoms formed along the axis of the aligned electrodes. The fact that the material fabricated in this process is made of carbon is checked through optical emission spectroscopy (OES), as will be explained in the following section. Conductive

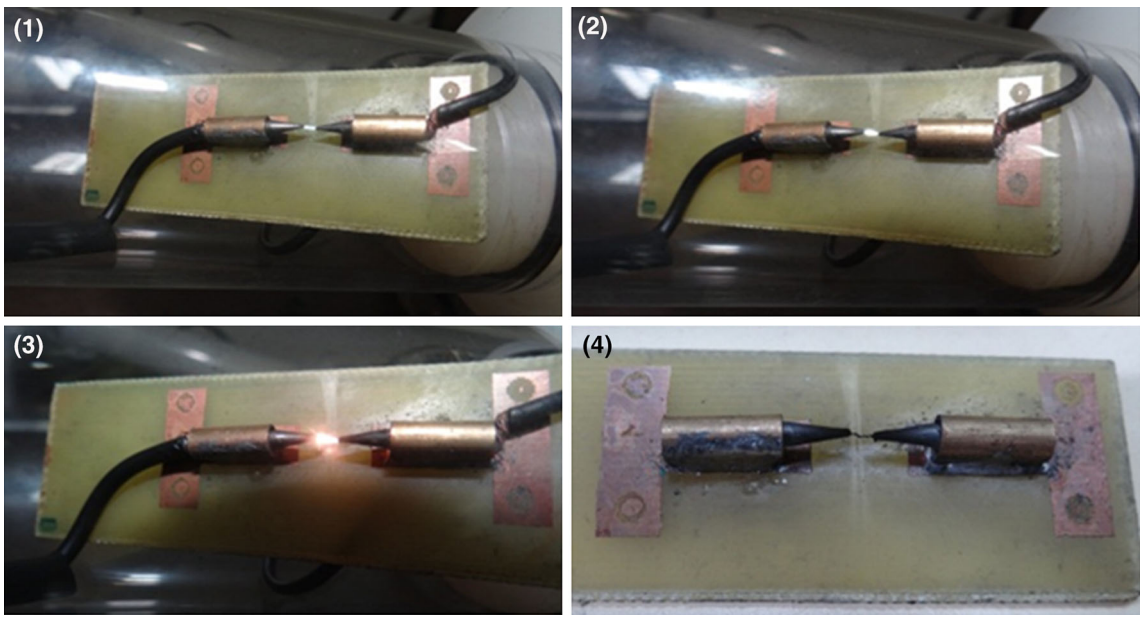

Fig. 2 Different states during the growth

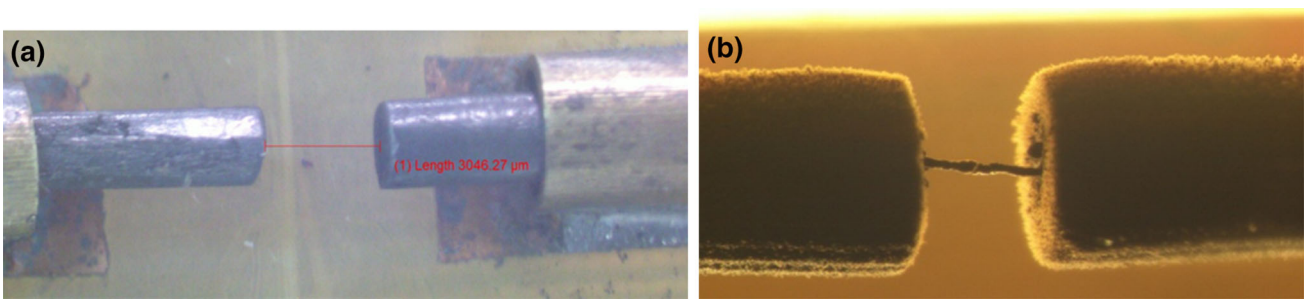

Fig. 3 Plane-to-plane configuration **a** before arc discharge decomposition and **b** after arc discharge decomposition and carbon strand developed

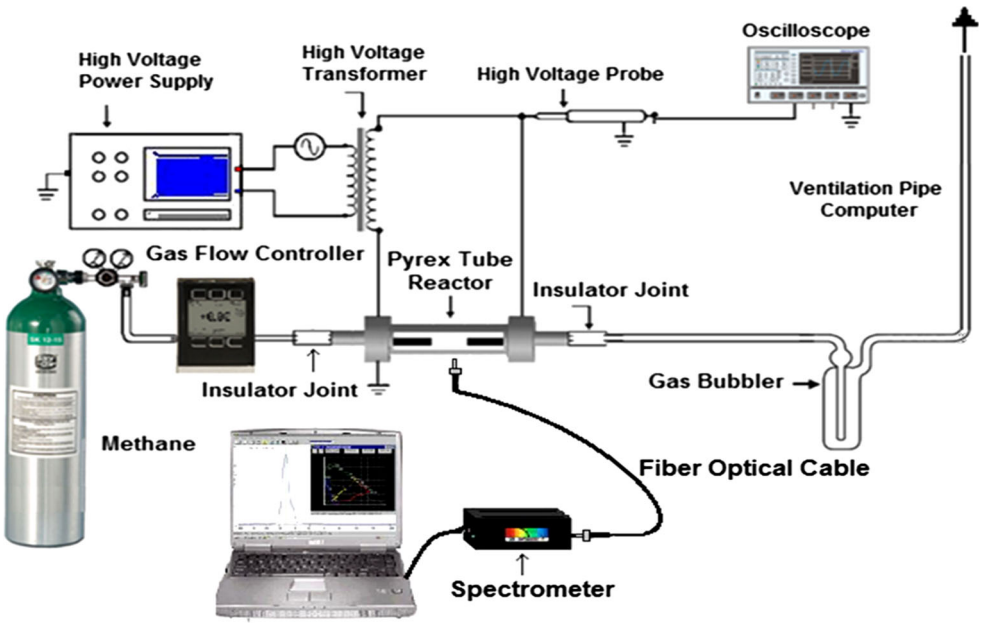

Fig. 4 Schematic for OES setup

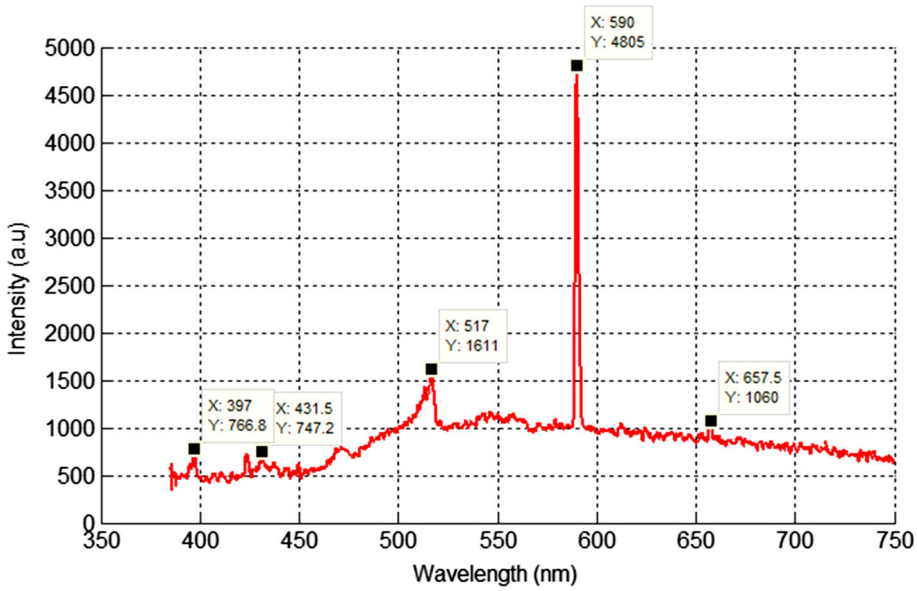

Fig. 5 Developed peaks of methane species

bridge is created by stacking the carbon atoms between two graphite electrodes when the arc discharge is started. As the carbon strand grows further and becomes thicker, the arc becomes weaker and less bright, i.e., the arc dims and gradually fades out while changing the color from bright blue to dark yellow. When the deposition is complete and the carbonaceous material has formed, the arc dies out completely. Figure 2 illustrates different states during the growth.

Table 2 The pure methane spices

Species	Wavelength (nm)	Energy (eV)
H_α	657.5	3.3
C_2	516.75	3.4
	590	–
CH	397	–
	431.4	2.9

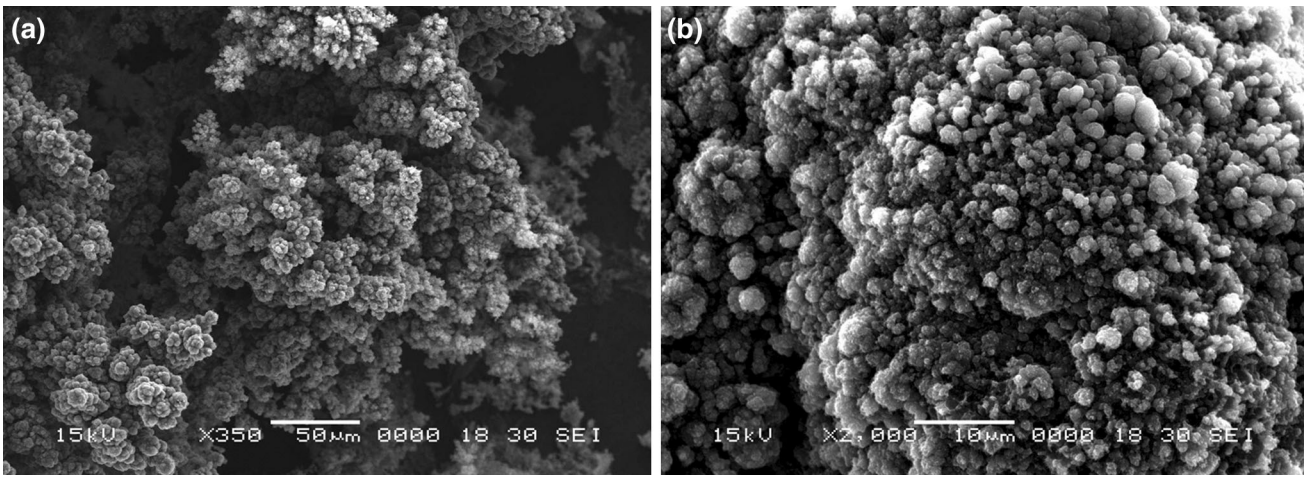

Fig. 6 SEM mode **a** X350 15 kV, **b** X2000 15 kV

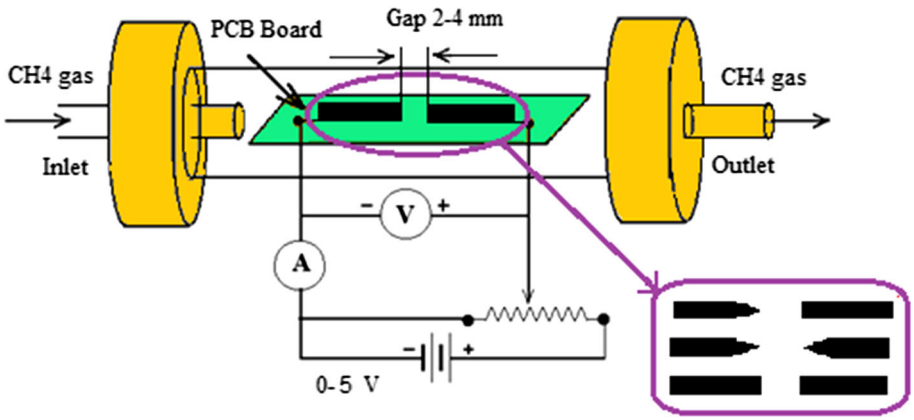

Fig. 7 Electrical measurement setup for the carbon strands

The carbon strand developed in the experiment was also inspected using optical microscope. Figure 3a, b shows the corresponding images obtained from high-resolution optical microscopy. The shape of the electrodes has significant effect on the electromagnetic field, which eventually influences the breakdown voltage, arc stabilization, and therefore the physiochemical process of depositions. There are three different configurations of graphite electrodes on the PCB board. These configurations are plane-to-plane (P–T–P), tip-to-plane (T–T–P), and tip-to-tip (T–T–T). Figure 3 illustrates the plane-to-plane electrode configuration.

OES is a technique used to detect and estimate the amount of various types of elements in different processes and environments. These include the metal contents in alloys and other elements in specific compound materials. This study implemented OES to ensure that the material produced during the methane decomposition is made of carbon. An illustration of the general configuration in which the devices have been connected and utilized in the experiment is provided in Fig. 4. As shown, the probe at the tip of the fiber optical cable has been in close contact with the Pyrex chamber and the spectrometer is connected to a computer in order to record the spectra emitted during the carbon growth state. This enables us to capture the spectra of the sparks ignited during the process to compare with those obtained in other works (Krcma et al. 2010; Patacsil et al. 2006). This will allow us to ensure that the material deposited between the electrodes is carbonaceous.

The wavelength range (385–750 nm) during carbon filming fabrication was recorded by spectrophotometer, and the captured data were drawn using MATLAB software.

As shown in Fig. 5, there are three developed peaks which belong to C_2, CH, and H_α. The appearance of the

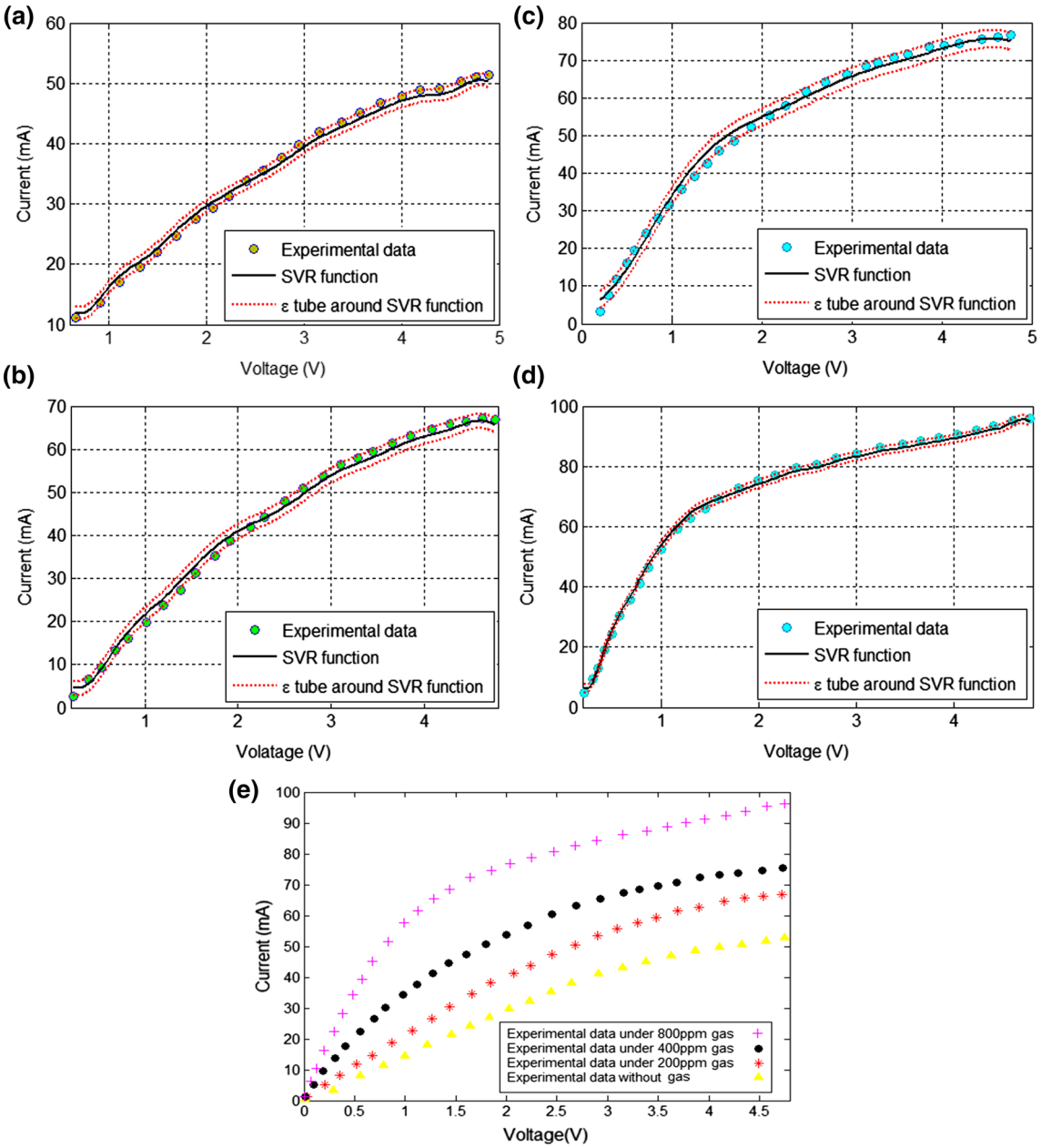

Fig. 8 SVR modeling **a** without CO_2 gas, **b** under 200 ppm, **c** 400 ppm, **d** 800 ppm, **e** all

peaks is revealed in Table 2. As illustrated in Fig. 5, the spectrum consists of phases of ionized species of methane which evolved. This indicates that peaks of CH appears at 397 and 431.4 nm, swan band C_2 appears at 516.75 nm, and hydrogen H_α appears at 657.5. These species represent the phenomenon of methane cracking under high voltage arc discharge conditions (Iqbal 2014).

The information about the composition and surface topography of the samples are provided by scanning electron microscopy (SEM) signals (Moon et al. 2009) as shown in Fig. 6a, b.

The carbon films exhibited electrical conductivity, which shows that the grown carbon film belongs to carbon nanotubes (CNTs), graphene, or graphite. Among all kinds

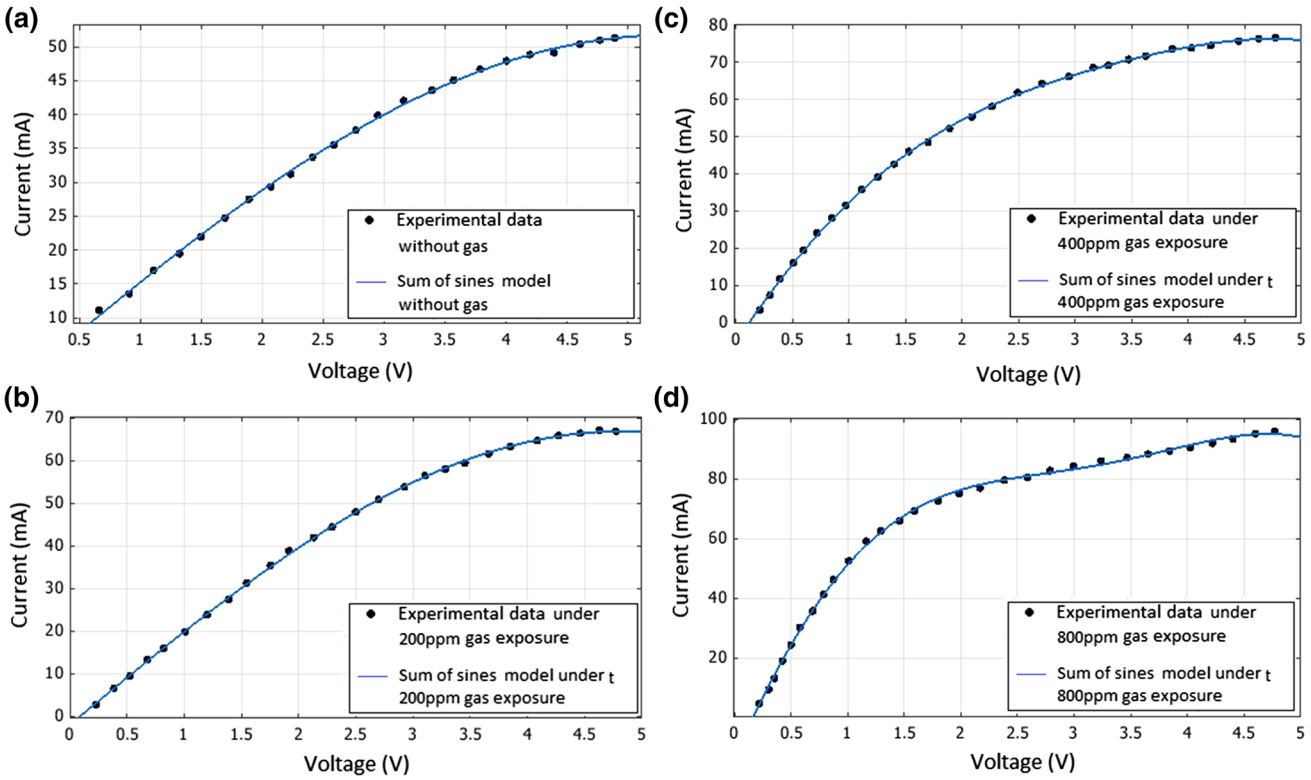

Fig. 9 Sum of sine model **a** without CO_2 gas, **b** under 200 ppm, **c** 400 ppm, **d** 800 ppm

of carbonaceous materials, the materials outlined above display conducting behavior. In addition, related images published in the literature (Lee et al. 2004; Patel 2011; Zhang et al. 2013) show that the material shown in the picture is made of carbon.

Electrical characterization of the grown carbon strand

Once the C-strands were produced, a series of low DC voltage measurements were taken on them in order to reveal their actual current–voltage characteristics. In doing this, a DC power supply was employed to apply low voltage to the two electrodes and the C-strand situated in between the electrodes. As shown in Fig. 7, the DC voltage (0–5 V) was applied to the graphite electrodes and the current measurement was taken with a microampere meter. The results are depicted in Figs. 8 and 9.

Support vector regression algorithm

In recent times, support vector regression (SVR) has been widely employed for prediction in chemical applications. SVR is another technique in computational intelligence associated with NN and is fundamentally based on the theory of statistical learning proposed by Vapnik. "Accordingly, (Anthony 1997; Cristianini and Shawe-Taylor 2000; Smola and Schölkopf 2004) have done some works based on SVR." In this research, we use the ε-SVR, which gives an approximate function $f(x)$. It therefore limits the deviations from the target y_i in the training data set $(i.e.\{(x_1, y_1)\ldots(x_I, y_L)\} \subseteq (X \times Y)^l)$ not to exceed a maximum value ε which makes it as flat as possible (Stahlbock and Lessmann 2004; Welling 2004). In other words, errors are neglected as long as they are smaller than a prespecified value ε. Unlike the ANN, training of the SVR includes convex optimization in which there are no local minima. "For instance, (Smola and Schölkopf 2004) used SVR and

Table 3 The selected values for ε, C, and γ

Dimension	Electrodes configuration	ε	C	γ
3 mm	PTP			
	Without gas	1	40.1685	0.3
	After 200 ppm gas exposure	1.7	64.4290	0.4
	After 400 ppm gas exposure	2.3	73.2046	0.8
	After 800 ppm gas exposure	1.3	91.2409	0.2

Table 4 Regressions and the corresponding values for a, b, and c parameters

Dimension	Electrodes configuration	a	b	c	SSE	R^2	RMSE
3 mm	PTP						
	Without gas	51.73	0.2922	0.0064	2.535	0.9993	0.356
	After 200 ppm gas exposure	66.86	0.3309	−0.03018	2.372	0.9998	0.3211
	After 400 ppm gas exposure	75.27	0.3707	0.04086	4.038	0.9987	0.419
	After 800 ppm gas exposure	94.37	0.3952	0.09186	19.17	0.9992	0.8937

ANN for optimization." A transformation function Φ is applied in the SVR algorithm to the original points to transform them from the initial input space to a feature space F of a higher dimension. In the obtained new space, a linear model is constructed corresponding to a nonlinear model in the original space. Thus, considering a simple linear problem, for this case, the transformation function is in the form of $f(x) = \langle w, \Phi(x)\rangle + b$ where $w \in X$ and $b \in \Re$. Here $\langle w, \Phi(x)\rangle$ represents the dot product of the input patterns x in the feature space. As a matter of fact, the support vectors are the data points which are used in the description of the searched function "For example (Gunn 1998) presented non-linear model." In the presence of noise, working with a soft margin obtained from the SVM would be more plausible. This can be evidently realized by slack variables ξ_i^-, $\xi_i^+ \geq 0$ with which the mathematical formulation can be extended in convex optimization (Smola and Schölkopf 2004),

$$\frac{1}{2}||W||^2 + C\sum_{i=1}^{l}\left(\xi_i^+ + \xi_i^-\right) \tag{1}$$

In order to ensure flatness, the equation above must be minimized by $||W||^2 = \langle w, w\rangle$ and applying the constraints $(w.\phi(x_i)) + b - y_i = \varepsilon + \xi_i^- y_i - (w.\phi(x_i)) - b \leq \varepsilon + \xi_i^+$. The constant C determines the trade-off between flatness and the amount of outliers of the ε-tube, which is handled in this study with the ε-intensive loss function "(Müller et al. 1997).

$$|\xi|_\varepsilon := \begin{cases} 0 & \text{if } |\xi| \leq \varepsilon \\ |\xi| \leq \varepsilon & \text{otherwise} \end{cases} \tag{2}$$

Employing the kernel function, one can derive a solution for the original regression problem, without the need to consider the transformation $\Phi(x)$ applied to the data explicitly. In this study, we have implemented radial basis functions (RBF). The accuracy of the model for the ε-SVR with RBF kernel function is dependent upon the parameters ε, C, and γ. As previously mentioned, the accuracy of the approximated function is determined by the magnitude of ε. For values of ε larger than the range of target data, expecting accurate results is a little over-optimistic. One can expect over-fitting for $\varepsilon = 0$. Thus, ε must be chosen in a way that it somehow reflects the data. The values of insensitivity function ε, and parameters C and γ were selected by trial-and-error method and are shown in Table 3.

Results and discussion

The changes observed in the current passing through the carbon strands as a result of voltage alterations were measured and recorded. These measurements were taken under gas exposure immediately after growth and also repeated several minutes (20 min) after growth in the absence of CO_2 gas. Also the I–V characteristics were measured for different varieties of carrier concentration (200,400, and 800 ppm).

And also SVR has been applied for prediction of the *I–V* characteristics without gas and under exposure to gas. The *I–V* readings are provided in Fig. 8a–e.

The most suitable empirical relation for our data processing can be written in the form

$$F(x) = a \times \sin(b \times x + c) \quad (3)$$

The parameters *a*, *b,* and *c* are recorded in Table 4.

Conclusion

Conclusively, the current–voltage characteristics of the carbon strands obtained were tested and evaluated in order to assess their potential ability to replace the channel in gas sensors. While applying a DC voltage to the carbon strands in successive time periods after the growth, the corresponding currents passing through the conductive channel was measured and recorded. The result shows changes in the carbon strand conductivity in the presence of gas, i.e., when the channel is exposed to gas, due to the absorption of gas atoms on the surface of the carbon strand, its conductivity increases. The SVR prediction method was implemented to provide a model for the *I–V* characteristics of the carbon strands before and after exposure to CO_2 gas. Afterward, the obtained model is capable of providing good estimations of the electrical behavior of the carbon strands. Therefore, this study proposes that carbon strand material can be used in gas detection sensors presenting high sensitivity, thus empowering sensor manufacturers to produce accurate sensing mechanisms in extremely smaller sizes.

Acknowledgments The authors would like to thank Ministry of Higher Education (MOHE), Malaysia (Grant Vot. No. 4F382), and the Universiti Teknologi Malaysia (Grants Vot. No. 03H86 and Postdoc Grant No. 02E11) for the financial support received during the investigation.

References

Akbari E, Ahmadi M, Yusof R, Ghadiry M, Saeidmanesh M (2013) Gas concentration effect on channel capacitance in graphene based sensors. J Comput Theor Nanosci 10(10):2449–2452

Akbari E, Buntat Z, Ahmad MH, Enzevaee A, Yousof R, Iqbal SMZ, Karimi H (2014a) Analytical calculation of sensing parameters on carbon nanotube based gas sensors. Sensors 14(3):5502–5515

Akbari E, Buntat Z, Enzevaee A, Mirazimiabarghouei SJ, Bahadoran M, Shahidi A, Nikoukar A (2014b) Correction: an analytical model and ANN simulation for carbon nanotube based ammonium gas sensors. RSC Adv 4(80):42581

Anthony M (1997) Computational learning theory. Cambridge University Press, Cambridge

Craig H, Chou C, Welhan J, Stevens C, Engelkemeir A (1988) The isotopic composition of methane in polar ice cores. Science 242(4885):1535–1539

Cristianini N, Shawe-Taylor J (2000) An introduction to support vector machines and other kernel-based learning methods. Cambridge University Press, Cambridge

Davidson EA, Ishida FY, Nepstad DC (2004) Effects of an experimental drought on soil emissions of carbon dioxide, methane, nitrous oxide, and nitric oxide in a moist tropical forest. Glob Change Biol 10(5):718–730

Gunn, S. R. (1998). Support vector machines for classification and regression. ISIS technical report 14

Gupta VK, Saleh TA (2013) Sorption of pollutants by porous carbon, carbon nanotubes and fullerene—an overview. Env Sci Pollut Res 20(5):2828–2843

Gupta VK, Ali I, Saleh TA, Nayak A, Agarwal S (2012) Chemical treatment technologies for waste-water recycling—an overview. RSC Adv 2(16):6380–6388

Gupta VK, Kumar R, Nayak A, Saleh TA, Barakat M (2013) Adsorptive removal of dyes from aqueous solution onto carbon nanotubes: a review. Adv Colloid Interface Sci 193:24–34

Huttunen JT, Alm J, Liikanen A, Juutinen S, Larmola T, Hammar T, Martikainen PJ (2003) Fluxes of methane, carbon dioxide and nitrous oxide in boreal lakes and potential anthropogenic effects on the aquatic greenhouse gas emissions. Chemosphere 52(3):609–621

Iqbal SMZ (2014) Decomposition of methane into carbonaceous material using arc discharge method. UTM thesis

Krcma F, Klohnova K, Polachova L, Horvath G (2010) Optical emission spectroscopy of abnormal glow discharge in nitrogen-methane mixtures at atmospheric pressure. Publications de l'Observatoire Astronomique de Beograd 89:371–374

Lee EK, Lee SY, Han GY, Lee BK, Lee T-J, Jun JH, Yoon KJ (2004) Catalytic decomposition of methane over carbon blacks for CO_2-free hydrogen production. Carbon 42(12–13):2641–2648

Moon YK, Lee J, Lee JK, Kim TK, Kim SH (2009) Synthesis of length-controlled aerosol carbon nanotubes and their dispersion stability in aqueous solution. Langmuir 25(3):1739–1743

Müller K-R., Smola AJ, Rätsch G, Schölkopf B, Kohlmorgen J, Vapnik V. (1997). Predicting time series with support vector machines artificial neural networks—ICANN'97 (pp. 999–1004): Springer

Patel N, Bazzanella RFN, Miotello A (2011) Enhanced hydrogen production by hydrolysis of NaBH4 using "Co-B nanoparticles supported on Carbon film" catalyst synthesized by pulsed laser deposition. Elsevier 170(1):20–26

Patacsil C, Malapit G, Ramos H (2006) Optical emission spectroscopy of low temperature CVD diamond. J Plasma Fusion Res Ser 7:145–149

Schoell M (1980) The hydrogen and carbon isotopic composition of methane from natural gases of various origins. Geochim Cosmochim Acta 44(5):649–661

Smola AJ, Schölkopf B (2004) A tutorial on support vector regression. Stat Comput 14(3):199–222

Stahlbock R, Lessmann S (2004) Potential von Support Vektor Maschinen im analytischen Customer Relationship Management. Universität Hamburg, Hamburg

Stevens CM, Engelkemeir A (1988) Stable carbon isotopic composition of methane from some natural and anthropogenic sources. J Geophys Res Atmos 93(D1):725–733

Welling M (2004) Support vector regression. Department of Computer Science, University of Toronto, Toronto

Zhang J, Jin L, Li Y, Si H, Qiu B, Hu H (2013) Hierarchical porous carbon catalyst for simultaneous preparation of hydrogen and fibrous carbon by catalytic methane decomposition. Int J Hydrog Energy 38(21):8732–8740